Organic LETTERS

Letter

pubs.acs.org/OrgLett

Deciphering the Origin of Stereoinduction in Cooperative Asymmetric Catalysis Involving Pd(II) and a Chiral Brønsted Acid

Garima Jindal and Raghavan B. Sunoj*

Department of Chemistry, Indian Institute of Technology Bombay, Powai, Mumbai 400076, India

Supporting Information

ABSTRACT: The density functional (M06) computations on a cooperative multicatalytic reaction involving palladium acetate and a chiral Brønsted acid in the conversion of an indenyl cyclobutanol to spirocyclic indene bearing a quaternary carbon ring junction are reported. A chiral Pd-*bis*-phosphate is identified as the active catalyst in the enantioselective ring expansion as compared to alternative possibilities wherein the chiral phosphate/phosphoric acid is in the outer sphere of palladium. The enantiocontrolling transition state exhibited more effective C−H···π interactions, lower distortion of the catalyst, and an orthogonal orientation of the bulky phosphate ligands.

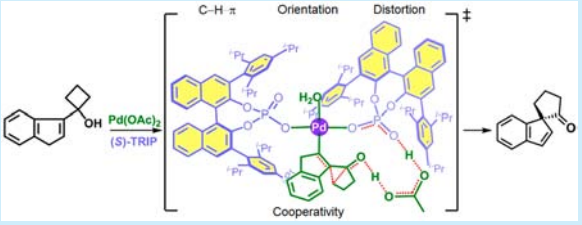

Cooperative asymmetric catalysis is a new and emerging trend in asymmetric synthesis.[1] The complementary attributes of both metal[2] and organocatalysts[3] are harnessed in the synthesis of increasingly complex molecules. The simultaneous use of two catalysts offers a handle to fine-tune the stereoselectivity by carefully choosing the chirality in one of the catalysts. Although there are reports on the use of multiple chiral catalysts in one-pot reactions, most of the recent examples in cooperative catalysis employ only one chiral catalyst in conjunction with an achiral catalyst. While several catalyst combinations can be thought of,[4] the metal-organo pair[1d,f] appears to be the most promising genre for asymmetric applications. The availability of several successful organocatalysts (such as chiral amines, N-heterocyclic carbenes, Brønsted acids, thiourea, etc.)[5] has certainly provided a timely impetus to metal-organo cooperative asymmetric catalysis. Needless to mention that transition metal catalysis has remained a central pillar in chemical catalysis for several decades. Hence, metal-organo cooperative protocols should be regarded as a natural progression on this front.

In a very recent example, Rainey et al. synthesized spirocyclic indenes by using a Pd−Brønsted acid dual catalytic method (Scheme 1).[6] The synthesis of spirocycles with chiral quaternary C-centers is an arduous task, and only a few methods are available to access such compounds.[7] Although Pd(II) and Brønsted acids are successful catalysts by themselves, the potential of their combination has not been exploited until recently. Some of the most recent examples using Pd−Brønsted acid dual catalytic combinations serve as an early indication of its incredible potential in cooperative catalysis.[8] Spirocyclic indenes are valuable compounds owing to their biological relevance and their use toward the development of spinol-based chiral ligands for asymmetric synthesis.[9] For instance, the basic framework of an antitumor antibiotic known as *fredericamycin-A* consists of a spirocyclic indene framework.[10] These features render the following reaction of high contemporary significance.

Scheme 1. Pd and Brønsted Acid Cooperative Catalytic Approach for the Formation of Spirocyclic Indenes (ref 6)

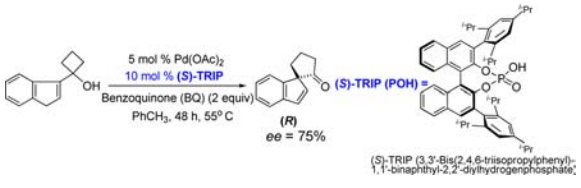

The conversion of indenyl cyclobutanol to spirocyclic indene, as given in Scheme 1, is accomplished by using (*S*)-TRIP (abbreviated, hereafter as POH) and $Pd(OAc)_2$ as the catalysts, BQ as the oxidant, and a trace of water as an additive, all under one-pot reaction conditions. Delineating the mechanism of such a dual catalytic reaction is expected to be challenging. The only chiral source in this reaction is the phosphoric acid, which is introduced as an *external* species, unlike what one would generally find in asymmetric catalysis wherein the chiral ligand is bound to the transition metal. Under such a scenario, the critical question of whether the chiral entity replaces the native ligand on palladium or does it imparts enantioselectivity by being in the outer coordination sphere of the metal warrants careful investigation.[11] In addition, the identification of what could possibly be the most preferred pathway requires knowledge of the nature of the active catalytic species and the preferred combination of the ligands bound to the Pd center.

Studies on the origin of stereoinduction undoubtedly demand mechanistic clarity. To this end, we have very recently established the mechanism of formation of the spirocyclic indene by using an achiral model phosphoric acid.[12] Two pathways, namely an allylic

Received: March 23, 2015
Published: June 9, 2015

DOI: 10.1021/acs.orglett.5b00860
Org. Lett. 2015, 17, 2874−2877

C−H activation and a Wacker-type pathway, were considered in great detail to learn that a Wacker-type mechanism is relatively more preferred. In the most preferred pathway, one H_2O and two phosphates are found to remain in the inner coordination sphere of Pd. In the present letter, we intend to shed light on the origin of enantioselectivity when a chiral (*S*)-TRIP acts as the Brønsted acid. The lowest energy pathway and the stereodetermining ring expansion step are shown in Scheme 2. Density functional

Scheme 2. A Wacker-Type Mechanism for the Formation of Spirocyclic Indene[a]

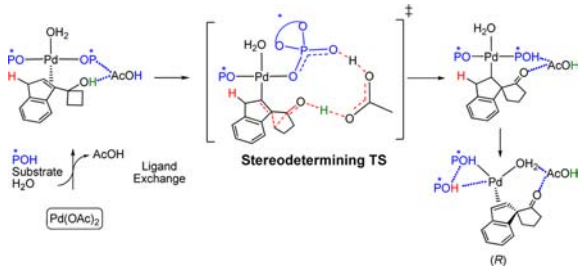

[a]The structure of POH is given in Scheme 1.

computations using the M06 functional have been employed to identify all the transition states involved in the stereodetermining step.[13] Discussions employ Gibbs free energies obtained at the $SMD_{(Toluene)}$/M06/6-311G**,LANL2DZ(Pd)//M06/6-31G**,LANL2DZ(Pd) level of theory, unless otherwise specified.

In the stereodetermining step, the chiral Brønsted acid could be envisaged as capable of playing different roles, as illustrated in Figure 1, depending on the nature of other bound ligands on Pd.

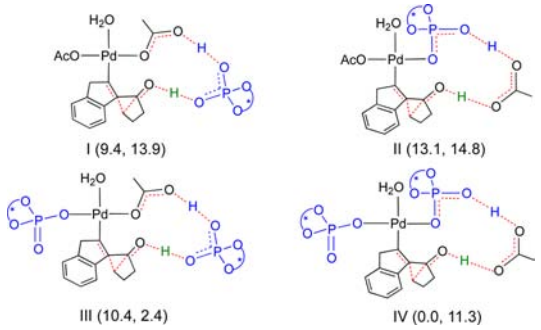

Figure 1. Different modes for the stereocontrolling transition states that differ in the nature of the ligands around Pd. Relative free energies (kcal/mol) with respect to the lowest energy transition state in mode **IV** are given in parentheses in the order (*si*, *re*). The *re* and *si* are the prochiral faces of the palladated indenyl framework.

For instance, with the native acetate ligands on Pd, the chiral phosphoric acid can remain only in the outer sphere bound through H-bonding interactions, depicted as mode **I** in Figure 1. Alternatively, the phosphoric acid can protonate and displace one of the acetates and move into the inner sphere as a phosphate, leading to modes **II** and **III**. Similarly, the action of two phosphoric acid molecules can give rise to a *bis*-phosphate intermediate, wherein the acetic acid is pushed to the outer sphere, as in mode **IV**.

Investigation of different possibilities for the stereocontrolling ring expansion step (modes **I**−**IV**) revealed that the transition state with two phosphate ligands, designated as mode **IV**, is energetically the most preferred. Within each of these transition state models, two stereochemically distinct ring expansions are considered. The migrating methylenic carbon can approach either the *si* face of the palladated indenyl framework, leading to an *R* spirocyclic indene, or the *re* face resulting in an *S* product. The vital controlling element for the developing chirality (or the extent of chiral induction) is the energy difference between the transition states for the migration to the *si* face and that to the *re* face. The relative Gibbs free energies of these transition states with respect to the lowest energy transition state in mode **IV** given in parentheses respectively pertain to the migrations to the *si* face (the first value) and the *re* face (the second value) (Figure 1). It can be readily noticed from Figure 1 that the transition states in modes **I** and **II** are generally of higher energy. Interestingly, within both these modes the lower energy transition state is the one that involves a migration to the *si* face, leading to the *R* product. This implies that the sense of selectivity obtained through these models is correct wherein the chiral phosphate is either directly bound to Pd (as in mode **II**) or it is H-bonded to other ligands (as in mode **I**). However, in the case of mode **III**, the predicted sense of selectivity is opposite to that from experimental observation, indicating that such a transition state model is much less likely.[14]

A few pertinent aspects on the increasing use of chiral phosphoric acids in transition metal catalysis are worth mentioning at this juncture.[1d,f] Under a homogeneous catalytic condition, the phosphoric acid can either act as a proton shuttle or protonate an anionic ligand bound to the transition metal to form a phosphate conjugate base. This phosphate, in turn, can act as an inner-sphere ligand to the transition metal or remain as a counterion in the outer-sphere.[15] Therefore, it is of fundamental importance to probe the actual role of the chiral phosphate/phosphoric acid in the stereocontrolling event of this reaction. Next, we turned our attention to the energetically most preferred transition state mode **IV** where the chiral phosphates act as ligands bound to the Pd. The predicted enantioselectivity with this transition state model is >99% due to the large energy difference (11.3 kcal/mol) between the diastereomeric transition states (Figure 2). A similar trend is also noticed with the B3LYP-D3//M06 level of theory (11.5 kcal/mol). The predicted value is therefore an overestimation of the enantioselectivity as compared to the experimental *ee* of 75%. At the B3LYP level, the free energy difference becomes −1.5 kcal/mol, in favor of the opposite stereoisomer (*R*). Further single-point calculations at the M06//B3LYP level of theory result in an energy difference of 7.4 kcal/mol. It appears that the M06 and B3LYP-D3 functionals tend to overestimate the C−H···π interactions leading to more stabilization of the lower energy transition state.[16] Careful analysis of the geometric features of this *bis*-phosphate transition state offered certain valuable molecular insights. The substrate is anchored to the Pd center while the stereocontrolling ring expansion takes place. The gross molecular topology indicates that the large spatial spread of the triisopropylphenyl arms extending from the 3,3′-positions of the axially chiral binaphthyl core is such that the substrate appears to remain encapsulated in the chiral pocket.[17] The relative orientation of the two phosphates in the lowest energy transition state **TS-*si*** is found to be nearly orthogonal to each other (Figure 2a), potentially leading to a minimization of the steric encumbrance.[18] In the higher energy **TS-*re***, in order for the *re* face of the indenyl framework to remain accessible for the ring expansion, the phosphates should have to reorient. This kind of substrate-induced conformational change, as shown in Figure 2a, leads to

DOI: 10.1021/acs.orglett.5b00860
Org. Lett. 2015, 17, 2874−2877

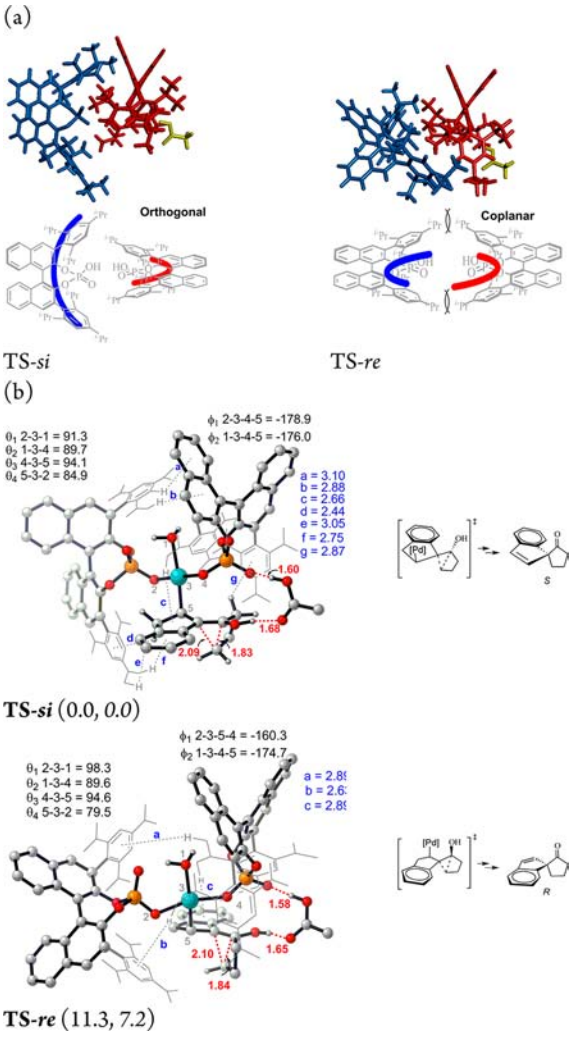

Figure 2. (a) Orientation of the two chiral phosphate ligands (shown in red and blue color) in the diastereomeric transition states in mode **IV**. The substrate and Pd are omitted for clarity. (b) Optimized geometries of the stereocontrolling transition states depicting noncovalent interactions. Relative Gibbs free energies (normal font) and total electronic energies (italics) in kcal/mol are given in parentheses. All distances are in Å, and angles in deg.

an increased steric interaction between the isopropyl groups of the two phosphate ligands.

Examination of the finer details, besides the seemingly evident steric interactions, reveals a series of weak C−H···π stabilizing interactions between the ligand and substrate.[19] The cumulative effect of these noncovalent interactions controls the geometric disposition of the substrate near the Pd center. It can be noticed from the optimized transition state geometries that the lower energy **TS-*si*** exhibits more C−H···π interactions (denoted as a to g in Figure 2b). The C−H···π contact distances in **TS-*si*** are generally shorter than those in **TS-*re***, indicating stronger interactions.[20] Another factor that contributes to the energy difference between the diastereomeric transition states is the geometry around the Pd atom, which is nearly square planar in the case of **TS-*si*** while larger distortions are noticed in **TS-*re***. A comparison of the distortion angles (θ_1−θ_4) and dihedral angles (ϕ_1−ϕ_2), as given in Figure 2b, effectively conveys a pronounced geometric distortion in the higher energy **TS-*re***.

It is interesting to note that the above-mentioned controlling factors responsible for the stereoinduction emanate from the crucial triisopropylphenyl groups on the chiral phosphate ligand. To quantify the stabilization/destabilization of transition states upon going from the original to the modified catalysts, different equations are formulated (Scheme 3). To probe the importance of the 3,3′ substituents on the binaphthol framework, the 3,3′ groups on the original catalyst (TRIP) are first replaced with H atoms, as shown in Scheme 3a. This is done for both stereodetermining TSs to evaluate the energy difference between the ring expansion involving the *si* and *re* face of the palladated indenyl framework. Single-point energies are first calculated using such frozen geometries. It is noticed that the energy difference between **TS-*si*** and **TS-*re*** dwindles to 0.2 kcal/mol as compared to 7.2 kcal/mol in the case of unmodified parent phosphate ligands.[21] Similarly, when all the triisopropylphenyl decorations on the 3,3′ aryl groups are replaced with just phenyl groups (Scheme 3b), the energy difference increases to 9.3 kcal/mol. Subsequently, the geometries of these transition states with the modified ligands as shown in Scheme 3 were allowed to relax by way of full geometry optimization at the M06/6-31G**,-LANL2DZ(Pd) level of theory.[22] Interestingly, the energy difference between the stereocontrolling transition states with Ar = H and that with Ar = C_6H_5 respectively became 0.9 and −1.5 kcal/mol (where Ar corresponds to the 3,3′ substituent on the binaphthyl core).[23] Thus, it is evident that the presence of isopropyl groups is of utmost importance to the enantioselectivity and the steric interactions between the isopropyl groups on the phosphate ligands, and the C−H···π stabilizing interactions

Scheme 3. Balanced Equations to Compare the Original Catalyst with the Modified Catalysts Obtained upon Replacing the 3,3′ Substituents with (a) Hydrogen Atoms and (b) Phenyl Groups (S = Substrate and AcOH = Acetic Acid)

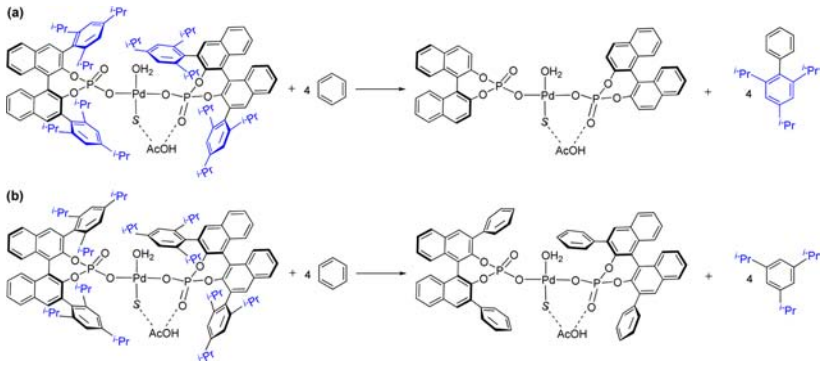

DOI: 10.1021/acs.orglett.5b00860
Org. Lett. 2015, 17, 2874−2877

between the ligand and the substrate are the prime contributing factors governing the stereochemical outcome.

In conclusion, we have proposed the first transition state model for a cooperative asymmetric Pd(II)-Brønsted acid catalyzed spirocyclic ring formation. In the stereodetermining transition state, both the transition metal and the Brønsted acid cooperatively participate in the enantioselective ring expansion transition state, wherein the methylenic carbon of the cyclobutanol migrates to the *si* prochiral face of the palladated indenyl carbon, to furnish a spirocyclic indene framework. In the lowest energy ring expansion mode involving the *si*-face, the chiral phosphate ligands remain nearly orthogonal so as to minimize the unfavorable steric interaction and at the same time engage in a series of weak stabilizing C−H···π interactions.

The ring expansion to the *re*-face, on the other hand, suffers from increased steric interactions between the triisopropylphenyl groups besides reduced C−H···π interactions. The higher computed ees appear to arise from the additivity of errors in the noncovalent interactions and thus allude to the challenges in quantitative predictions for larger catalysts. The molecular insights presented herein could help in the rational design of cooperative catalytic protocols involving palladium acetate in conjunction with chiral phosphoric acids.

■ ASSOCIATED CONTENT

Supporting Information

Cartesian coordinates of all the transition states. The Supporting Information is available free of charge on the ACS Publications website at DOI: 10.1021/acs.orglett.5b00860.

■ AUTHOR INFORMATION

Corresponding Author

*E-mail: sunoj@chem.iitb.ac.in.

Notes

The authors declare no competing financial interest.

■ ACKNOWLEDGMENTS

IIT Bombay computer center, some additional computing resources at the National Nanotechnology Infrastructure Network at Michigan, and a senior research fellowship (G.J.) from CSIR (New Delhi) are acknowledged.

■ REFERENCES

(1) (a) Paull, D. H.; Abraham, C. J.; Scerba, M. T.; Alden-Danforth, E.; Lectka, T. *Acc. Chem. Res.* **2008**, *41*, 655. (b) Allen, A. E.; MacMillan, D. W. C. *Chem. Sci.* **2012**, *3*, 633. (c) Xu, H.; Zeund, S. J.; Woll, M. G.; Tao, Y.; Jacobsen, E. N. *Science* **2010**, *327*, 986. (d) Rueping, M.; Koenigs, R. M.; Atodiresei, I. *Chem.—Eur. J.* **2010**, *16*, 9350. (e) Raup, D. E. A.; Cardinal-David, B.; Holte, D.; Scheidt, K. A. *Nat. Chem.* **2010**, *2*, 766. (f) Du, Z.; Shao, Z. *Chem. Soc. Rev.* **2013**, *42*, 1337. (f) Chen, D.-F.; Han, Z.-Y.; Zhou, X.-L.; Gong, L.-Z. *Acc. Chem. Res.* **2014**, *47*, 2365. (g) Jindal, G.; Kisan, H. K.; Sunoj, R. B. *ACS Catal.* **2015**, *5*, 480.

(2) (a) Desimoni, G.; Faita, G.; Jørgenson, K. A. *Chem. Rev.* **2011**, *111*, PR284. (b) Wu, X.-F.; Fang, X.; Wu, L.; Jackstell, R.; Neumann, H.; Beller, M. *Acc. Chem. Res.* **2014**, *47*, 1041. (c) Liu, X.; He, L.; Liu, Y.-M.; Cao, Y. *Acc. Chem. Res.* **2014**, *47*, 793. (d) Tang, R.-Y.; Li, G.; Yu, J.-Q. *Nature* **2014**, *507*, 215. (e) He, J.; Li, S.; Deng, Y.; Fu, H.; Laforteza, B. N.; Spangler, J. E.; Homs, A.; Yu, J.-Q. *Science* **2014**, *343*, 1216.

(3) (a) Maruoka, K.; List, B.; Yamamoto, H.; Gong, L.-Z. *Chem. Commun.* **2012**, *48*, 10703. (b) List, B.; Yang, J. W. *Science* **2006**, *313*, 1584. (c) Mukherjee, S.; Yang, J. W.; Hoffmann, S.; List, B. *Chem. Rev.* **2007**, *107*, 5471. (d) MacMillan, D. W. C. *Nature* **2008**, *455*, 304. (e) Volla, C. M. R.; Atodiresei, I.; Rueping, M. *Chem. Rev.* **2014**, *114*, 2390. (f) Akiyama, T. *Chem. Rev.* **2007**, *107*, 5744.

(4) For metal−metal, see: (a) Nakao, Y.; Yada, A.; Hiyama, T. *J. Am. Chem. Soc.* **2010**, *132*, 10024. (b) Park, J.; Hong, S. *Chem. Soc. Rev.* **2012**, *41*, 6931. For organo−organo, see: (c) Uraguchi, D.; Ueki, Y.; Ooi, T. *Science* **2009**, *326*, 120. (d) Zhao, X.; DiRocco, D. A.; Rovis, T. *J. Am. Chem. Soc.* **2011**, *133*, 12466.

(5) *Comprehensive Enantioselective Organocatalysis: Catalysts, Reactions, and Applications*; Dalko, P. I., Ed.; Wiley-VCH Verlag GmbH & Co. KGaA: Weinheim, Germany, 2013.

(6) Chai, Z.; Rainey, T. J. *J. Am. Chem. Soc.* **2012**, *134*, 3615.

(7) (a) Wang, B.; Tu, Y. Q. *Acc. Chem. Res.* **2011**, *44*, 1207. (b) Franz, A. K.; Hanhan, N. V.; Ball-Jones, N. *ACS Catal.* **2013**, *3*, 540. (c) D'yakonov, V. A.; Trapeznikova, O. A.; de Meijere, A.; Dzhemilev, U. M. *Chem. Rev.* **2014**, *114*, 5775.

(8) (a) Yip, K.-T.; Nimje, R. Y.; Leskinen, M. V.; Pihko, P. M. *Chem.—Eur. J.* **2012**, *18*, 12590. (b) Zhang, S.-Y.; He, G.; Nack, W. A.; Zhao, Y.; Li, Q.; Chen, G. *J. Am. Chem. Soc.* **2013**, *135*, 2124. (c) Yu, S.-Y.; Zhang, H.; Gao, Y.; Mo, L.; Wang, S.; Yao, Z.-J. *J. Am. Chem. Soc.* **2013**, *135*, 11402. (d) Osberger, T. J.; White, M. C. *J. Am. Chem. Soc.* **2014**, *136*, 11176.

(9) (a) Wang, X. M.; Han, Z. B.; Wang, Z.; Ding, K. L. *Angew. Chem., Int. Ed.* **2012**, *51*, 936. (b) Xie, J.-H.; Zhou, Q.-L. *Acc. Chem. Res.* **2008**, *41*, 581.

(10) (a) Albel, U.; Simon, W.; Eckard, P.; Hansske, F. G. *Bioorg. Med. Chem. Lett.* **2006**, *16*, 3292. (b) Kita, Y.; Higuchi, K.; Yoshida, Y.; Iio, K.; Kitagaki, S.; Ueda, K.; Akai, S.; Fujioka, H. *J. Am. Chem. Soc.* **2001**, *123*, 3214.

(11) Jindal, G.; Sunoj, R. B. *J. Org. Chem.* **2014**, *79*, 7600.

(12) Jindal, G.; Sunoj, R. B. *J. Am. Chem. Soc.* **2014**, *136*, 15998.

(13) (a) All calculations were done using Gaussian09. See the Supporting Information (SI) for full details. (b) Frisch, M. J. et al. *Gaussian 09*, Revision A.02; Gaussian, Inc.: Wallingford, CT, 2004.

(14) For details of higher energy modes, see Figure S1 of the SI.

(15) (a) We have recently established the role of chiral Brønsted acids in a Pd catalyzed asymmetric allylation reaction and Rh catalyzed N−H insertion. While in the former case the counterion participated in the stereodetermining step, the stereoselectivity in the latter was controlled by the Brønsted acid. (b) Reference 11. (c) Kisan, H. K.; Sunoj, R. B. *Chem. Commun.* **2014**, *50*, 14639.

(16) (a) Krenske, E. H.; Houk, K. N.; Lohse, A. G.; Antoline, J. E.; Hsung, R. P. *Chem. Sci.* **2010**, *1*, 387. (b) Zhang, W.; Zhu, Y.; Wei, D.; Li, Y.; Tang, M. *J. Org. Chem.* **2012**, *77*, 10729.

(17) For an illustration of the substrate fit to the chiral cavity of the catalyst, a space-filling model of the lower energy TS is provided in Figure S2 of the SI.

(18) The number of likely conformers is found to be severely restricted due to the larger aryl groups. While we have made the best attempts to sample important conformers of both transition states, the existence of other conformers cannot be fully eliminated. For higher energy conformers, see Figure S3 in the SI.

(19) For a recent example of noncovalent interaction (C−H···π) driven asymmetric induction, see: Jindal, G.; Sunoj, R. B. *Angew. Chem., Int. Ed.* **2014**, *53*, 4432.

(20) Topological analysis using the Atoms-In-Molecule (AIM) formalism indicates higher electron densities at the bond critical points for these interactions. See Figure S4 and Table S1 in the SI.

(21) Single-point energy computations were done at the SMD$_{(Toluene)}$/M06/6-311G**,LANL2DZ(Pd)//M06/631G**,-LANL2DZ(Pd) level of theory.

(22) (a) The transition states when 3,3′ positions are occupied by hydrogens and phenyl groups are given in Figure S5 of the SI. (b) Substitution of the 3,3′ substituents with H-atoms resulted in destabilization of both diastereomeric transition states whereas corresponding substitution with phenyl groups resulted in stabilization of the higher energy **TS-*re*** and destabilization of the lower energy **TS-*si***. For additional details see Figure S6 in the SI.

(23) An overlap of the original catalyst and the modified catalysts is given in Figure S7 of the SI.

DOI: 10.1021/acs.orglett.5b00860
Org. Lett. 2015, 17, 2874−2877